ACS OMEGA

http://pubs.acs.org/journal/acsodf

Article

Liquefaction of Lignin Using Chemical Decomposition and Its Application to Polyurethane Foam

Jisu Jeong, Woo Sik Kim, Min Wook Lee, and Munju Goh*

Cite This: *ACS Omega* 2021, 6, 10745−10751

Read Online

ACCESS | Metrics & More | Article Recommendations | Supporting Information

ABSTRACT: To utilize the chemical application of lignin (LN), a decomposition reaction was carried out to cleave chemical bonds. Indeed, a liquefaction process is essential for the chemical use of lignin to achieve a uniform reaction and maximize the chemical utility of lignin. To this end, hydroxyl radicals were adopted as a powerful oxidation agent, and FT-IR results confirmed the cleavage of the ether linkages. Additionally, the water solubility of LN significantly increased after decomposition, and dissolution levels up to 0.5 g·mL^{-1} were obtained. Using these high solubility properties in water, NMR and DLS analyses were performed. In particular, an average particle diameter of 300 ± 240 nm was found, corresponding to the size of polydisperse *l*-LN. By controlling size uniformity and using high water-solubility levels, polyurethane foams were manufactured using *l*-LN.

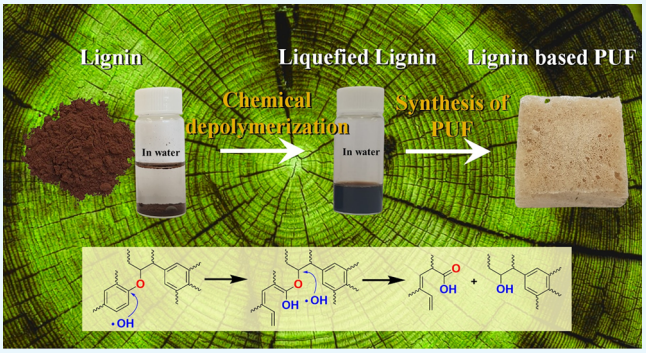

1. INTRODUCTION

Lignin (LN) is an abundant natural polymer within the wood sector and a byproduct of the paper process. Chemically, LNs are cross-linked phenolic polymers in which aromatic compounds are connected in a three-dimensional network structure. Owing to this phenolic-like network structure, it is both insoluble and infusible; therefore, it is often regarded as an impurity and discarded because of difficulties in industrial use.[1] The current global production of LN is ca. 630 000 t·year^{-1}, the majority of which is combusted for heat recovery, a low-value utilization. However, if LNs rich in aromatic compounds and hydroxyl groups can be utilized chemically, it would establish a novel natural resource, and many studies to this end are being conducted.

Since solid LN makes a nonuniform dispersion state in a solvent, the uniformity of the reaction cannot be obtained in the application through a chemical reaction. Thus, a liquefaction process is essential for the chemical use of lignin to achieve a uniform reaction. To date, several technologies have been studied for the direct liquefaction of lignin, including pyrolysis, solvolysis with organic solvents, and hydrothermal liquefaction with water.[2−4] These reactions cleave the chemical bonds of LN using high thermal energy. Accordingly, thermochemical depolymerization using water and an organic solvent was carried out in an inert environment at high temperatures (150−350 °C) and pressures (5−25 MPa).[5−7] Additional studies on the liquefaction of LN have been performed by attaching substituent groups, such as flexible glycerol or poly(ethylene glycol), to the hydroxy group of rigid LN, or using hydrogenation under mild conditions.[5−7]

A primary obstacle to the chemical use of biomaterials is the difficulty in controlling the uniformity of a product due to natural differences in molecular weight that vary with the growth process. Thus, as a complement to the two methods described above, there is an increasing demand for chemical treatment methods that can ensure uniformity and solubility by decomposing LN under mild conditions.

Polyurethane (PU) foam is a polymer material that is used in a variety of applications such as furniture, car seats, and insulation.[8] PU foams are synthesized by the polyaddition reaction between polyols and isocyanates. However, the monomers used to synthesize these PU foams are mostly derived from petroleum.[9] The interest and popularity of biodegradable and renewable biobased raw materials are increasing to solve the environmental problems caused by the use of fossil resources. Recently, biobased polyols are being studied for the production of sustainable and ecofriendly PU foams such as lignin.[10] Lignin is an important and desirable candidate for petroleum replacement. Due to its reproducibility, low cost, and rich and unique chemical structure such as rigid cyclic compounds, research studies are actively underway

Received: January 16, 2021
Accepted: April 9, 2021
Published: April 19, 2021

https://doi.org/10.1021/acsomega.1c00285
ACS Omega 2021, 6, 10745−10751

Scheme 1. Liquefaction Procedure of LN with Chemical Decomposition

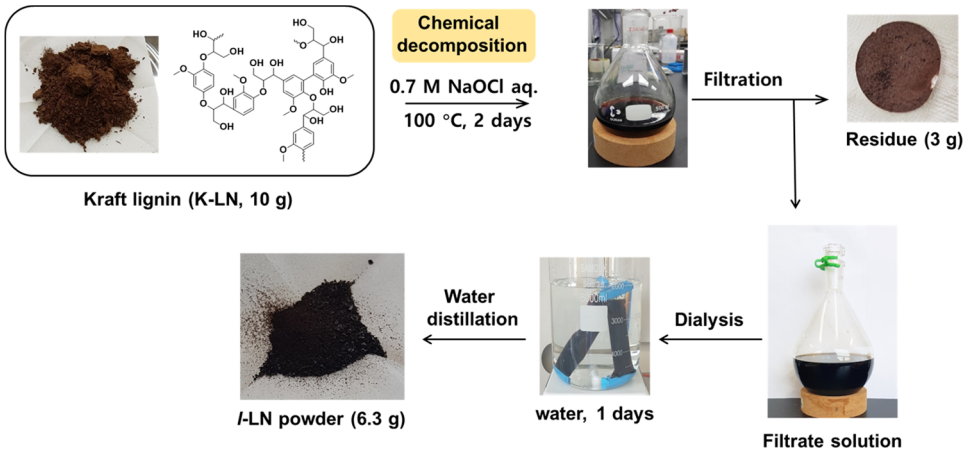

as a promising polymeric material for the production of biobased PU foam.[11]

In the present study, the decomposition reaction of high-molecular-weight LN was carried out using hydroxyl radicals that maintain strong oxidation power under mild conditions. Liquefied lignin with excellent solubility and stability in an aqueous solution was obtained, and chemical analyses were conducted using nuclear magnetic resonance (NMR) and infrared (IR) spectroscopy. In addition, polyurethane foam (PUF) using liquefied lignin was synthesized, demonstrating its potential use as an insulating material.

2. EXPERIMENTAL METHODS

2.1. Materials and Characterization. Kraft lignin (K-LN) was purchased from Sigma-Aldrich. It contains 5% moisture and loses 3.3 wt % at temperatures >149 °C. Sodium hypochlorite (9−11%) was purchased from Daejung Chemical Co. (Korea), poly(propylene glycol) (PPG) and (diol type) 700 were purchased from Wako Pure Chemical (Japan), and tin(II) 2-ethylhexanoate and toluene diisocyanate (2,4-, *ca.* 80%; 2,6-, *ca.* 20%) were purchased from Tokyo Chemical Industry Co. (Japan). Excess diisocyanate, beyond the quantity required to react with the OH− groups of the PPG, was reacted with distilled water to form CO_2, which acts as a blowing agent.[12] A dialysis membrane (Cellu-Sep; MFPI Company) was used to exclude molecular weights <3500 g·mol^{-1}.

2.1.1. Fourier Transform Infrared Spectroscopy (FT-IR). FT-IR spectra were measured using a JASCO FT-IR spectroscope (FT-IR 4100; Japan). LN was measured in a solid powder form, and the spectra were recorded with a resolution of 4 cm^{-1} and 32 scans per sample across the range of 4000−700 cm^{-1}.

2.1.2. Dispersion Stability. The dispersion stability of the liquified LN powder (*l*-LN) was evaluated using a Turbiscan LAB (Formulaction, France). Samples of 0.1 and 0.3 g·mL^{-1} of *l*-LN (aq.) were prepared for evaluation. The Turbiscan methodology consists of measuring backscatter and transmission intensities versus the sample height (*ca.* 50 mm), as a function of time (120 min).

2.1.3. Proton Nuclear Magnetic Resonance (NMR) Spectroscopy. Proton NMR analyses of *l*-LN were carried out at 500 MHz on a JEOL 500 spectrometer (Japan) with a D_2O solvent. The pulse width was 1 μs and delay time was 2 s. The number of scans was 124 on *ca.* 10 mg of the *l*-LN powder dissolved in deuterium oxide and packed into a glass sample tube.

2.1.4. Dynamic Light Scattering (DLS). DLS experiments were carried out using a Zetasizer Nano (Malvern Panalytical, U.K.), with scattered light intensity maintained at 90° and a temperature of 298 K.

2.1.5. Thermogravimetric Analysis (TGA). TGA was performed on the solid-state samples by means of a TGA (NETZSCH Instruments, TG209 F3; Germany) from ambient temperature to 900 °C at a scan rate of 20 °C·min^{-1} in a nitrogen atmosphere.

2.1.6. Scanning Electron Microscopy (SEM). An AJSM5600LV SEM (JEOL; Japan) was used to study the morphology of samples sputtered using an Edwards Sputter Coater.

2.1.7. Thermal Conductivity Evaluation. A hot disk TPS 2500 thermal constant analyzer (ThermTest Inc., Canada) was used to measure thermal conductivity, thermal diffusivity, and volumetric heat capacity according to the transient plane source method. Three separate measurements were performed for each PUF sample. The heating power was set to 20 mW, and a frequency of 60 Hz and a measurement time of 40 s were used as the testing parameters.

2.1.8. Flame Retardancy. To evaluate the flame-retardant properties, microscale combustion calorimeter (MCC) tests were carried out using an FAA Micro Calorimeter. The samples were heated to 750 °C at a heating rate of 1 °C·s^{-1} in an atmosphere of nitrogen 80% and oxygen 20%.

2.2. Liquefaction of LN with Chemical Decomposition. All chemical reagents and solvents were used in the commercially available state without further purification. The liquefaction reaction using chemical depolymerization was carried out under standard atmospheric conditions. LN (10 g) was placed in a 500 mL round-bottom flask fitted with a reflux condenser, after which distilled water (100 mL) and NaOCl (100 mL, 0.7 M) were added. The reaction mixture was refluxed at 100 °C for 48 h. It should be mentioned that the chemical depolymerization reaction was carried out at a boiling point of water at 100 °C. In addition, the reaction proceeded in 48 h when all of the LN precipitate disappeared during the reaction. As the reaction proceeded, the gradual change of the solution to a dark brown color confirmed the dissolution of the agglomerated LN. Following the reflux period, the reaction mixture was vacuum filtered and washed several times with distilled water. The filtered LN residue was dried at 100 °C in

https://doi.org/10.1021/acsomega.1c00285
ACS Omega 2021, 6, 10745−10751

a vacuum oven for 2 h and 3 g of undecomposed LN was recovered. The filtrate solution (*i.e.*, *l*-LN) was placed into a dialysis tube, and the sealed tube was stirred in a distilled water bath for 24 h. Finally, water was removed from the *l*-LN in the dialysis tube through distillation and 6.3 g of the LN powder was obtained. Excluding 5 wt % moisture in 10 g of K-LN, 0.2 g of LN less than 3500 g·mol^{-1} was excluded in the dialysis process and 6.3 g of *l*-LN was obtained. That is, at a rate of 66.3%, *l*-LN having a molecular weight greater than 3500 g·mol^{-1} was synthesized. It should be noted that the obtained LN powder was abbreviated as *l*-LN for convenience because it readily produces a liquefied LN solution when dissolved again into water. All of the liquefaction procedures with chemical decomposition are shown in Scheme 1.

2.3. Stoichiometric Analysis of *l*-LN. The hydroxyl and acid numbers of *l*-LN were evaluated to determine the stoichiometric ratio of functional groups that can react with isocyanates during polyurethane (PU) synthesis.

2.3.1. Hydroxyl Number of l-LN. The hydroxyl number of *l*-LN was determined as follows: a mixture of 1 g *l*-LN and 25 mL of a phthalation reagent was heated for 20 min at 110 °C. This was followed by the addition of 50 mL of 1,4-dioxane and 25 mL of distilled water, and the mixture was titrated with a 1 M sodium hydroxide solution to the equivalence point using a pH meter. The phthalation reagent consisted of a mixture of 150 g of phthalic anhydride, 24.2 g of imidazole, and 1000 g of 1,4-dioxane. The hydroxyl number in mg KOH·(g of sample)$^{-1}$ was calculated using the following equation

$$\text{hydroxyl number (mmol·g}^{-1}) = \frac{(B - A) \times N}{W}$$

where A is the volume of the sodium hydroxide solution required for the titration of the *l*-LN sample (mL), B is the volume of the blank solution (mL), N is the normality of the sodium hydroxide solution (g·mL^{-1}), and W is the weight of *l*-LN (g).

2.3.2. Acid Number of l-LN. A mixture of 0.8 g of the *l*-LN sample, 8 mL of 1,4-dioxane, and 2 mL of deionized water was titrated with a 1 M sodium hydroxide solution to the equivalence point. The acid number in mg KOH·(g of sample)$^{-1}$ was calculated using the following equation

$$\text{acid number (mmol·g}^{-1}) = \frac{(C - B) \times N}{W}$$

where C is the titration volume of the sodium hydroxide solution at the equivalence point (mL).

2.3.3. NCO:OH Ratio for PUF. The amount of isocyanate required was estimated using the following equation

$$\frac{\text{NCO}}{\text{OH}} = \frac{M_{\text{NCO}} W_{\text{NCO}}}{\left[M_{\text{OH}} W_{\text{OH}} + M_{\text{l-LN}} W_{\text{l-LN}} + \left(\frac{2}{18}\right) W_{\text{H}_2\text{O}}\right]} \times 100$$

where M_{NCO} is the number of isocyanate groups in 2 g of isocyanate, W_{NCO} is the weight of isocyanate (g), M_{OH} is the number of hydroxyl groups contained in 1 g of polyol (poly(propylene glycol) 700, *i.e.*, PPG 700), W_{OH} is the weight of polyols (g), $M_{\text{l-LN}}$ is the number of hydroxyl groups contained in the weight of *l*-LN, $W_{\text{l-LN}}$ is the weight of *l*-LN (g), and $W_{\text{H}_2\text{O}}$ is the weight of water.

2.4. Synthesis of PUF Including *l*-LN. A PUF system composed of diol-type polyol (PPG 700), tin(II) catalysts, *l*-LN powder (0, 1, 1.5, 3, and 6 wt % in 1 g of PPG 700), and distilled water (0.6 mL) were hand mixed until the *l*-LN powder was fully dissolved. Then, toluene diisocyanate (2 g) was added to the reaction mixture and mixed until bubbling. The reaction mixture was then poured into a 50 × 50 × 20 mm^3 mold lined with aluminum foil and the lid of the mold was quickly closed. The mold was placed in an oven for 1 h at 80 °C.[14] This preparation process for synthesizing PUFs is shown in Scheme S1.

3. RESULTS AND DISCUSSION

3.1. Characterization of the *l*-LN Powder. The chemical composition of the *l*-LN powder was determined by FT-IR spectroscopy, TGA, and ^{1}H NMR. Figure 1 shows the FT-IR

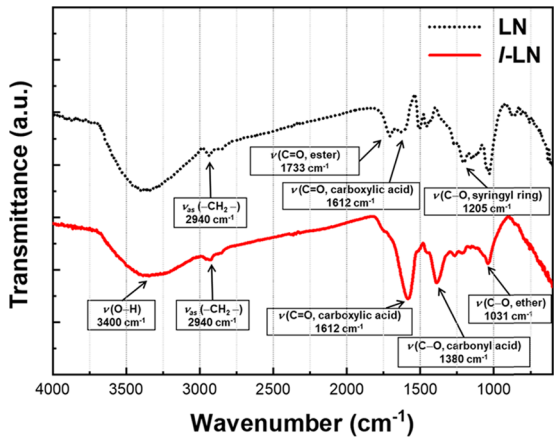

Figure 1. FT-IR results of LN (dotted black line) and *l*-LN (solid red line).

results for LN and *l*-LN, and the absorption peaks correspond to the C−O vibration of ether (1031 cm^{-1}), C−O vibration of the syringyl ring of LN (1205 cm^{-1}), C−O vibration of carboxylic acid (1380 cm^{-1}), C═O vibration of carboxylic acid (1612 cm^{-1}), C═O vibration of ester (1733 cm^{-1}), −CH_2− stretching of aliphatic compounds (2940 cm^{-1}), and −OH stretching (3400 cm^{-1}). Interestingly, the peak intensity of the C−O vibration derived from the syringyl ring of LN was notably decreased in *l*-LN.

In contrast, the characteristic peaks derived from the C═O and C−O vibration of carboxylic acid were remarkably increased in *l*-LN.[11] These results indicate that the carbonyl peak (C−O) of the ether linkage of LN at 1205 cm^{-1}, typically observed with a low peak derived from the syringyl ring of LN, is cleaved to carboxylic acid during chemical decomposition, leading to strong peaks of C═O and C−O in *l*-LN. This is further corroborated by the acid number obtained in the stoichiometric analysis of *l*-LN, 3.51 mmol·g^{-1}, notably higher than that of K-LN (2 mmol·g^{-1}).[12] Based on the FT-IR and acid number analyses, the plausible chemical decomposition reaction mechanism of LN is presented in Scheme 2.

Hydroxyl radicals have a strong oxidation potential and can cause oxidation reactions under mild conditions. Presently, hydroxyl radicals are used to break down various natural products, such as glucose and lignin, and even chemically stable ether linkages can be cleaved into carboxylic acids and alcohols through oxidation reactions.[13−17] In the present study, NaOCl was used as the source of the hydroxyl radical. It is believed that NaOCl (aq.) liberates hydroxyl radicals under

https://doi.org/10.1021/acsomega.1c00285
ACS Omega 2021, 6, 10745−10751

Scheme 2. (Upper) Plausible Chemical Decomposition Reaction Mechanism of LN and (Lower) Solubility Test Photographs of LN (Left) and *l*-LN (Right) in Water

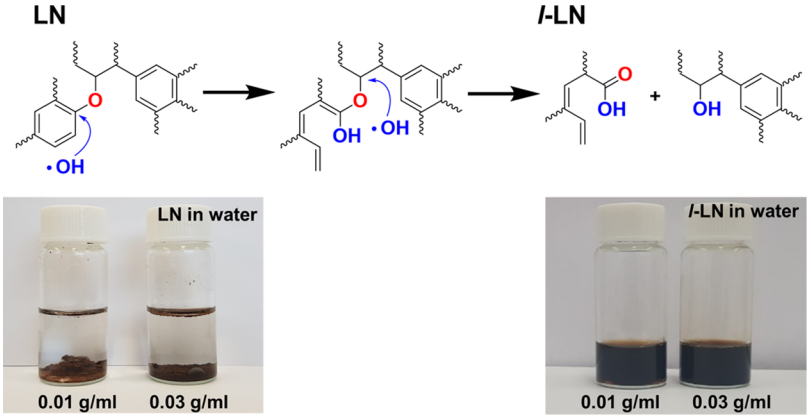

mild conditions, and the generated radicals cleave the ether linkage of the syringyl ring into carboxylic acid and alcohol via oxidization. As a result, it was confirmed that LN, which is water insoluble, becomes soluble after oxidization (*i.e.*, *l*-LN) is water soluble (Scheme 2). It was confirmed through the Turbiscan measurement that *l*-LN with a concentration of 0.01 and 0.03 g·mL^{-1} in water showed excellent dispersion stability for 24 h (Figure 2). Moreover, the maximum dissolved concentration of *l*-LN obtained was 0.5 g·mL^{-1}.

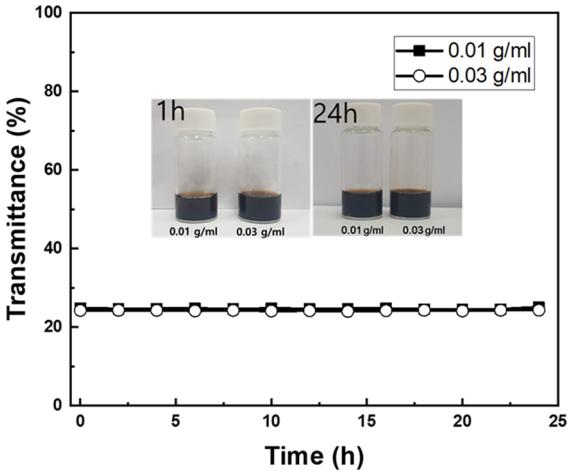

Figure 2. Turbiscan profile of transmittance changes with *l*-LN concentrations of 0.01 and 0.03 g·mL^{-1} in water. Scans were performed every 2 h for 24 h. Photographs after 1 and 24 h are presented in the inset.

By virtue of the good water solubility of *l*-LN, NMR and DLS measurements were possible and the molecular structure and particle sizes of *l*-LN could be predicted (Figure S1 presents the NMR results). Protons of the aromatic ring (Ar−H) of *l*-LN were observed between the 7.0 and 8.0 ppm region. The *α*-hydrogens of the ether group (−O−CH$_2$−) were observed between 3.2 and 4.6 ppm and aliphatic compounds and protons (−CH$_2$−) appeared in a multipeak form between 0.5 and 2.8 ppm. The DLS (Figure 3) illustrated an average particle diameter of 300 ± 240 nm (±1 SD), indicating polydispersity. To the best of the author's knowledge, this is the smallest particle size of wood-derived LN and is >3 times smaller than the particle size of LN (1000 nm at 0.01 g·mL^{-1})

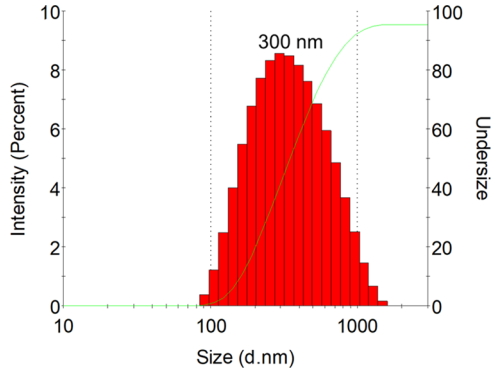

Figure 3. DLS results of *l*-LN (0.01 g·mL^{-1}) particle-size distribution.

obtained from sugarcane.[18−22] In the case of K-LN, the particle size could not be measured using DLS because it is water insoluble.

Figure 4 shows the TGA and DTG results for LN and *l*-LN. During the heating procedure, LN showed three distinct peaks

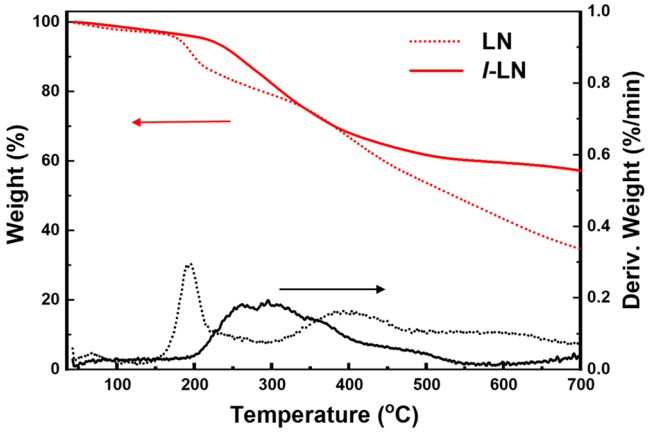

Figure 4. TGA (red lines) and DTG (black lines) results of LN (dotted lines) and *l*-LN (solid lines).

around 100−200, 200−500, and 500−700 °C. It was thought that the first weight loss (*ca.* 5 wt % loss) around 25−200 °C was attributable to the vaporization of residual moisture in the sample, and the second weight loss (*ca.* 37 wt % loss) was the decomposition of hydroxyl and aliphatic functional groups. Finally, the 28 wt % loss observed around 500−700 °C was

https://doi.org/10.1021/acsomega.1c00285
ACS Omega 2021, 6, 10745−10751

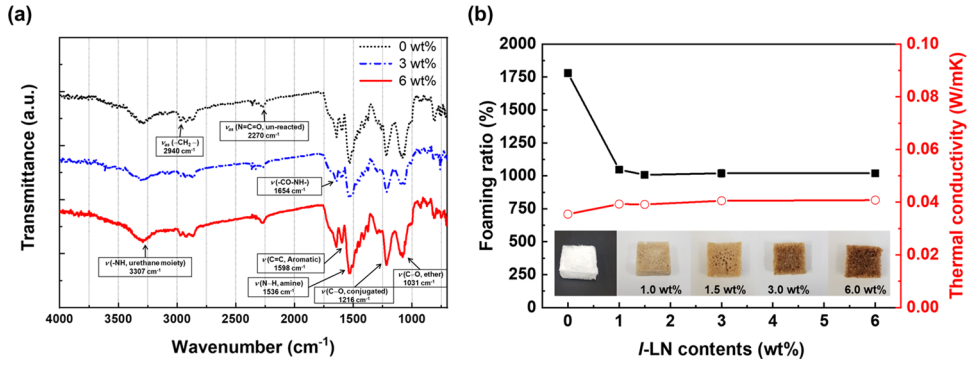

Figure 5. (a) FT-IR results of *l*-LN-containing PUFs. (b) Changes in the foaming ratio (black line) and thermal conductivity (red line) of PUFs, correlated with various *l*-LN concentrations. A photograph of the PUFs formed can be seen in the inset.

mainly attributed to the loss of ether groups and protons in LN. As a result, 28 wt % of the char yield at 700 °C was observed in LN. Comparatively, only a single peak was observed in the TGA results of *l*-LN at approximately 200−650 °C. Similar to LN, a weight loss of *ca.* 5 wt % was observed between 100 and 200 °C due to moisture, and approximately 30 wt % loss was observed at *ca.* 200−650 °C due to the hydroxyl and aliphatic functional groups. A high char yield of *ca.* 55 wt % at 700 °C was observed in the TGA of *l*-LN. This unexpectedly high value is thought to be due to the relatively small weight loss at 200−600 °C in the thermal decomposition of *l*-LN, as ether and the small molecular aliphatic groups were already removed during chemical decomposition.

3.2. Application of *l*-LN to PUF. We prepared water-blown PUF by utilizing *l*-LN that was uniformly soluble in water. When synthesizing PU copolymers, hydroxyl groups can be combined with isocyanate monomers to form cross-links and the CO_2 generated by the reaction of excess diisocyanate and water can be used as a blowing agent.[14] To find the optimal conditions for making PUF before adding *l*-LN, the types of monomers (aliphatic or aromatic diisocyanate), monomer amount, catalyst's presence or absence, water content, and creaming time were investigated (Figure S2).

FT-IR spectra of the *l*-LN-containing PUFs were utilized to study their chemical structure (Figure 5a). Absorption peaks were found corresponding to the −NHCOO− vibration of urethane linkage (1654 cm^{-1}), C═C stretching of the aromatic ring in *l*-LN (1598 cm^{-1}), −N−H bending (1536 cm^{-1}), and C−O stretching (1216 cm^{-1}).[23,24] PUF foaming ratios correlated with various levels of *l*-LN content were also evaluated. The foaming ratio was determined by the expanded volume based on the sum of the volumes of each monomer. The initial foaming ratio was *ca.* 1780% but it decreased to *ca.* 1100% after the addition of *l*-LN (Figure 5b). This is likely due to the increase in the total −OH of the reaction system derived from the addition of *l*-LN, which increases the consumption of diisocyanate. Stated another way, the relative amount of diisocyanate that can react with water decreases, which reduces the amount of CO_2 produced and used as the blowing agent. Nevertheless, even when the content of *l*-LN was increased to 6 wt %, the foaming ratio was *ca.* 1100%. Thermal conductivity is closely related to cell morphology, and SEM images of *l*-LN-containing PUFs can be seen in Figure S5. Typical cellular structures were observed on the cross-sectional surfaces of all PUFs. As shown in Figure 5b, the thermal conductivities of the *l*-LN-containing PUFs were between 0.035 and 0.041 $W{\cdot}mK^{-1}$ at 0−6 wt % *l*-LN content.

Figure 6 shows the char yield *l*-LN-containing PUFs with increasing *l*-LN contents. As the *l*-LN content increases from 0

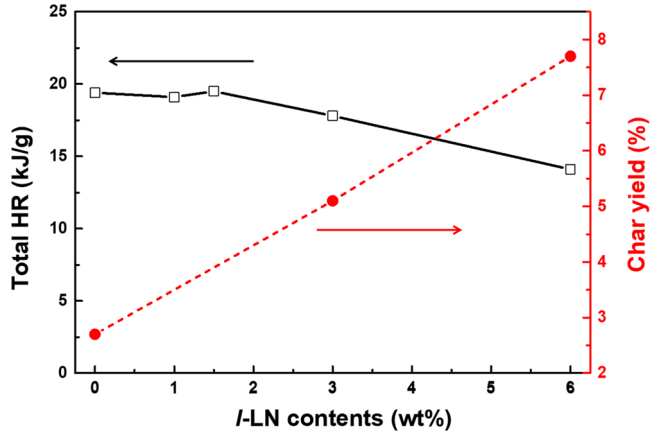

Figure 6. Char yield and total HR properties as *l*-LN contents for *l*-LN-containing PUFs.

to 6 wt %, the char yield also increases from 2.7 to 7.7%, respectively. Microcalorimetry measurement was carried out to investigate the fire behavior of *l*-LN-containing PUFs. The heat-release rate (HRR) measured by a microcalorimeter is a very important parameter as the HRR peak value is used to express the intensity of a fire. The HRR result demonstrates that the addition of *l*-LN leads to a reduction in the HRR, which decreases from 19.4 $kJ{\cdot}g^{-1}$ for the neat PUF to 14.1 $kJ{\cdot}g^{-1}$ for 6 wt % *l*-LN-containing PUF, with a reduction of 27.3%.

4. CONCLUSIONS

Lignin (LN) is an abundant, natural, cross-linked phenolic polymer; however, due to this phenolic-like network structure, it is both insoluble and infusible. Because of these properties, the chemical utility of LN is extremely limited. Recently, many effective methods of LN liquefaction have been developed and their chemical utilization has improved. However, since the chemical bonds of LN could not be broken until now, uniform quality of chemical application was elusive owing to the chemical state of LN containing highly variable molecular weights. To address this problem, we adopted a chemical decomposition reaction using hydroxyl radicals as strong oxidation agents for the cleavage of LN linkages, and the cleavage of the ether linkage was apparent from the FT-IR results. Furthermore, after the chemical decomposition

https://doi.org/10.1021/acsomega.1c00285
ACS Omega 2021, 6, 10745−10751

reaction, the water solubility of LN was significantly enhanced and we succeeded in dissolving concentrations up to 0.5 g·mL^{-1} without substituting the functional groups. To the best of the authors' knowledge, this value is the highest solubility level attainable for pure LN in water. NMR and DLS analyses were possible using this increase in solubility. In particular, it was found that the average particle diameter of polydisperse *l*-LN was 300 ± 240 nm (1 SD), a value nearly three times smaller than that reported in the literature. By controlling size uniformity and using highly soluble *l*-LN in water, we succeeded in manufacturing PUFs. In the future, this method can maximize the utility of LN in producing chemical products with various uniform properties.

■ ASSOCIATED CONTENT

Supporting Information

The Supporting Information is available free of charge at https://pubs.acs.org/doi/10.1021/acsomega.1c00285.

NMR analysis of liquefied lignin, synthetic routes for PUF, and SEM results of PUFs (PDF)

■ AUTHOR INFORMATION

Corresponding Author

Munju Goh − *Department of Chemical Engineering, Konkuk University, Seoul 05029, Republic of Korea;* orcid.org/0000-0002-6061-8625; Email: mgoh@konkuk.ac.kr

Authors

Jisu Jeong − *Department of Chemical Engineering, Konkuk University, Seoul 05029, Republic of Korea*

Woo Sik Kim − *Fibrous Ceramics & Aerospace Materials Center, Korea Institute of Ceramic Engineering & Technology, Jinju-si, Gyeongsangnam-do 52851, Republic of Korea*

Min Wook Lee − *Institute of Advanced Composite Materials, Korea Institute of Science and Technology, Bongdong-eub, Jeonbuk 55324, Republic of Korea;* orcid.org/0000-0003-3256-1067

Complete contact information is available at: https://pubs.acs.org/10.1021/acsomega.1c00285

Notes

The authors declare no competing financial interest.

■ ACKNOWLEDGMENTS

This research was supported by Basic Science Research Program through the National Research Foundation of Korea (NRF) funded by the Ministry of Education (Grant No. 2020R1F1A1049281), and this research was supported by Human Resources Program in Energy Technology of the Korea Institute of Energy Technology Evaluation and Planning (KETEP), granted financial resource from the Ministry of Trade, Industry & Energy, Republic of Korea. (Grant No. 20194010201790), and this work was also supported by the Technology Innovation Program (No. 20012817) funded by the Ministry of Trade, Industry & Energy (MOTIE, Korea).

■ REFERENCES

(1) *Lignin Chemistry*; Serrano, L.; Luque, R.; Sels, B.; Agirre, I., Eds.; Springer, 2020.

(2) Laird, D. A.; Brown, R. C.; Amonette, J. E.; Lehmann, J. Review of the pyrolysis platform for coproducing bio- oil and biochar. *Biofuels, Bioprod. Biorefin.* **2009**, *3*, 547−562.

(3) Alam, D.; Lui, M. Y.; Yuen, A.; Maschmeyer, T.; Hanynes, B. S.; Montoya, A. Reaction Analysis of Diaryl Ether Decomposition under Hydrothermal Conditions. *Ind. Eng. Chem. Res.* **2018**, *57*, 2014−2022.

(4) Jensen, M. M.; Djajadi, D. T.; Torri, C.; Rasmussen, H. B.; Madsen, R. B.; Venturini, E.; Vassura, I.; Becker, J.; Iversen, B. B.; Meyer, A. S.; Jørgensen, H.; Fabbri, D.; Glasius, M. Hydrothermal Liquefaction of Enzymatic Hydrolysis Lignin: Biomass Pretreatment Severity Affects Lignin Valorization. *ACS Sustainable Chem. Eng.* **2018**, *6*, 5940−5949.

(5) Bernardini, J.; Cinelli, P.; Anguillesi, I.; Coltelli, M. B.; Lazzeri, A. Flexible polyurethane foams green production employing lignin or oxypropylates lignin. *Eur. Polym. J.* **2015**, *64*, 147−156.

(6) Xue, B. L.; Wen, J. L.; Sun, R. C. Lignin-Based Rigid Polyurethane Foam Reinforced with Pulp Fiber: Synthesis and Characterization. *ACS Sustainable Chem. Eng.* **2018**, *6*, 5940−5949.

(7) Chen, L.; Muyden, A. P.; Cui, X.; Laurenczy, G.; Dyson, P. J. Selective hydrogenation of lignin-derived compounds under mild conditions. *Green Chem.* **2020**, *22*, 3069−3073.

(8) Gómez-Fernández, S.; Ugarte, L.; Correas, T. C.; Rodriguez, C. P.; Corcuera, M. A.; Eceiza, A. Properties of flexible polyurethane foams containing isocyanate functionalized kraft lignin. *Ind. Crops Prod.* **2017**, *100*, 51−64.

(9) Agrawal, A.; Kaur, R.; Walia, R. S. PU foam derived from renewable sources: Perspective on properties enhancement: An overview. *Eur. Polym. J.* **2017**, *95*, 255−274.

(10) Upton, B. M.; Kasko, A. M. Strategies for the Conversion of Lignin to High-Value Polymeric Materials: Review and Perspective. *Chem. Rev.* **2016**, *116*, 2275−2306.

(11) Leskinen, T.; Kelley, S. S.; Argyropoulos, D. S. Refining of Ethanol Biorefinery Residues to lsolate Value Added Lignins. *ACS Sustainable Chem. Eng.* **2015**, *3*, 1632−1641.

(12) Cinelli, P.; Anguillesi, I.; Lazzeri, A. Green synthesis of flexible polyurethane foams from liquefied lignin. *Eur. Polym. J.* **2013**, *49*, 1174−1184.

(13) Bernardini, J.; Anguillesi, I.; Coltelli, M. B.; Cinelli, P.; Lazzeri, A. Optimizing the lignin based synthesis of flexible polyurethane foams employing reactive liquefying agents. *Polym. Int.* **2015**, *64*, 1235−1244.

(14) Kim, D. H.; Lee, M.; Goh, M. Enhanced and Eco-Friendly Recycling of Carbon-Fiber-Reinforced Plastics Using Water at Ambient Pressure. *ACS Sustainable Chem. Eng.* **2020**, *8*, 2433−2440.

(15) Ruiz, H. A.; Cerqueira, M. A.; Silva, H. D.; Rodríguez-Jasso, R. M.; Vicente, A. A.; Teixeira, J. A. Biorefinery valorization of autohydrolysis wheat straw hemicellulose to be applied in a polymer-blend film. *Carbohydr. Polym.* **2013**, *92*, 2154−2162.

(16) Boeriu, C. G.; Bravo, D.; Gosselink, R. J. A.; van Dam, E. G. Characterization of structure-dependent functional properties of lignin with infrared spectroscopy. *Ind. Crops Prod.* **2004**, *20*, 205−218.

(17) He, W.; Gao, W.; Fatehi, P. Oxidation of Kraft Lignin with Hydrogen Peroxide and its Application as a Dispersant for Kaolin Suspensions. *ACS Sustainable Chem. Eng.* **2017**, *5*, 10597−10605.

(18) Liu, C.; Wu, S.; Zhang, H.; Xiao, R. Catalytic oxidation of lignin to valuable biomass-based platform chemicals: A review. *Fuel Process. Technol.* **2019**, *191*, 181−201.

(19) Li, H.; Bunrit, A.; Li, N.; Wang, F. Heteroatom-participated lignin cleavage to functionalized aromatics. *Chem. Soc. Rev.* **2020**, *49*, 3748−3763.

(20) Zhou, L.; Yang, X.; Xu, J.; Shi, M.; Wang, F.; Chen, C.; Xu, J. Depolymerization of cellulose to glucose by oxidation-hydrolysis. *Green Chem.* **2015**, *17*, 1519−1524.

(21) Hafezisefat, P.; Lindstorm, J. K.; Brown, R. C.; Qi, L. Non-catalytic oxidative depolymerization of lignin in perfluorodecalin to produce phenolic monomers. *Green Chem.* **2020**, *22*, 6567−6578.

(22) Posoknistakul, P.; Tangkrakul, C.; Chaosuanphae, P.; Deepentham, S.; Techasawong, W.; Phonphirunrot, N.; Bairak, S.; Sakdaronnarong, C.; Laosiripojana, N. Fabrication and Character-

ization of Lignin Particles and Their Ultraviolet Protection Ability in PVA Composite Film. *ACS Omega* **2020**, *5*, 20976−20982.
(23) Kumari, S.; Chauhan, G. S.; Monga, S.; Kaushik, A.; Ahn, J. H. New ligin-based polyurethane foam for wastewater treatment. *RSC Adv.* **2016**, *6*, 77768−77776.
(24) Mahmood, N.; Yuan, Z.; Schmidt, J.; Tymchyshyn, M.; Xu, C. Hydrolytic liquefaction of hydrolysis lignin for the preparation of bio-based rigid polyurethane foam. *Green Chem.* **2016**, *18*, 2385−2398.

https://doi.org/10.1021/acsomega.1c00285
ACS Omega 2021, 6, 10745−10751